Journal of Applied Polymer Science

Method for Time–Temperature–Transformation Diagrams Using DSC Data: Linseed Aliphatic Epoxy Resin

Nora Catalina Restrepo-Zapata,[1] Tim A. Osswald,[2] Juan P. Hernández-Ortiz[1,3]

[1]Departamento de Materiales, Universidad Nacional de Colombia, Calle 75 # 79A-51, Bloque M17, Medellín, Colombia

[2]Department of Mechanical Engineering, Polymer Engineering Center, University of Wisconsin-Madison, Madison, Wisconsin 53706-1691

[3]Biotechnology Center, University of Wisconsin-Madison, Madison, Wisconsin 53706-1691

Correspondence to: J. P. Hernández-Ortiz (E-mail: jphernandezo@unal.edu.co) or (E-mail: jphernandezo@wisc.edu)

ABSTRACT: A novel method to generate time–temperature–transformation (TTT) diagrams from Differential Scanning Calorimetry (DSC) data is presented. The methodology starts with dynamical DSC information to obtain the total transformation heat, followed by an isothermal-dynamic temperature ramp that allows the inclusion of diffusion-controlled reaction kinetic. The cure kinetics is modeled using an auto-catalytic Kamal–Sourour model, complemented with a Kissinger model that allows the direct prediction of one energy of activation, DiBenedetto's equation for the glass transition temperature as a function of the cure degree and adjusted reaction constants to include diffusion mechanisms. The methodology uses a nonlinear least-squares regression method following J.P. Hernández-Ortiz and T.A. Osswald's methodology (J. Polym. Eng. 2004, 25, 23). A typical linseed epoxy resin (EP) presents two different kinetics control mechanisms, thereby providing a good model to validate the proposed experimental and theoretical method. TTT diagrams for EPs at two different accelerator concentrations are calculated from direct integration of the kinetic model. © 2014 Wiley Periodicals, Inc. J. Appl. Polym. Sci. **2014**, *131*, 40566.

KEYWORDS: crosslinking; Differential Scanning Calorimetry; kinetics; thermosets

Received 9 December 2013; accepted 4 February 2014

DOI: 10.1002/app.40566

INTRODUCTION

Thermoset resins are polymers that change irreversibly under the influence of heat, light, or photomechanical agents. They pass from a meltable and soluble material to nonmeltable and insoluble through the formation of a three-dimensional covalent network.[1–3] This molecular structure results in high mechanical, thermal, and chemical properties, making it suitable to many applications in engineering. In addition, thermoset resins have low shrinkage, good dimensional and thermal stability, good chemical resistance, good electrical properties, and excellent adhesion properties.[4,5]

Epoxy resins (EPs) are the most common high-performance thermoset polymer matrices used today in advanced composites.[1–3,6–8] Due to their performance properties, they are extensively used as coatings, adhesives, laminates, and electronic encapsulants and in structural applications, which require lightweight and high strength. EPs are usually composed of short polymeric molecules, known as oligomers, which contain a minimum of two epoxide groups and a curing agent. The curing agent, also known as the hardener, is commonly an amide. The curing agent reacts with the epoxide functional groups through a ring-opening addition polymerization. Due to the size of the oligomers, hardened epoxies come as a compact and densely crosslinked structure. An EP may contain cyclic or internal epoxide groups but most of the time they are found to be terminal. Figure 1 presents a typical epoxide resin: the diglycidyl ether of bisphenol-A. This epoxy is produced by the reaction of Bisphenol A with epichlorohydrin in presence of sodium hydroxide.[9]

Due to the fact that the functionality of reactants controls the development and the crosslinked density of the network, it is possible to tailor and improve epoxy properties for specific applications, that is, selecting curing agents, epoxy molecules, and additives. In addition, fillers such as short fibers, metallic or inorganic particles, and various minerals can also be used in multiple applications.[10–16] It is important to fully understand the effects of fillers and additives during the curing process, and it is fundamental to know the processability window of these resins to optimize part design, properties, and performance. Novel experimental and theoretical methods that provide a

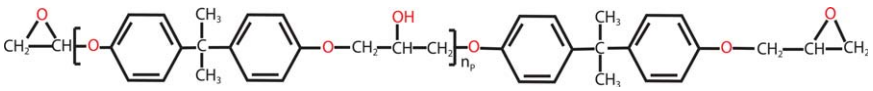

Figure 1. Molecular structure of the epoxy diglycidyl ether of bisphenol-A with *nP* polymeric repeating units. [Color figure can be viewed in the online issue, which is available at wileyonlinelibrary.com.]

better understanding of structure-property relationships would generate new avenues for material design and applications.

Physical, mechanical, and electrical properties of a thermosetting polymer are directly related to the degree of cure. The processability of a thermoset resin critically depends on the rate and extent of polymerization under specific processing conditions. Therefore, kinetic characterization of the reactive resin is not only important for a better understanding of structure-property relationships, but it is also fundamental in optimizing process conditions and product quality.[17–22] To make optimum use of epoxies as structural materials, it is important to know how the curing process evolves, to what extent the transformation proceeds, the cured material structure and how all these variables are influenced and limited by temperature.

The cure kinetics is a complex phenomena and includes several steps: at the beginning there is a linear formation and growth of polymer chains, then branching begins and the real crosslinking occurs at the end. During the process, macromolecules are linked by chemical bonds (covalent and/or ionic) and a network with high density of crosslinks is obtained. This structure restricts the relative movement between molecules and they do not flow after reheating. These reactions are exothermic and irreversible.[1,23–25] In general, the cure kinetics can be described by the reaction between two chemical groups denoted as A and B, which link two chemical groups of the polymeric chain. The dynamic scanning of the concentration of A and/or B can monitor the reaction. Thus, the cure (or transformation) degree can be defined as follows,[26–28]

$$c = \frac{C_{A_0} - C_A}{C_{A_0}} \tag{1}$$

where C_A is the concentration of A, C_{A_0} is the initial concentration of A, and c is the cure degree. To estimate the transformation directly from this equation is difficult, because it requires a direct measurement of the concentrations of A and/or B during the process. Numerous experimental techniques to study resin cure rates have been reported in the literature with emphasis on the chemical, physical, and mechanical property changes during cure.[29] Most of the techniques are limited due to the difficulty in handling a curing resin system as it changes from a liquid to a solid state. For example, infrared transmittance measurements have been used to follow the chemical changes occurring in a curing resin system. These are more sensitive at the early stages of the process, where the rate of chemical reaction is the highest.[30,31] Dynamic mechanical analysis[32,33] permits the cure process to be monitored on a macroscopic level by measuring the elastic and loss moduli as the resin changes from liquid to rubber and eventually to glass. Another lesser extent techniques used to characterize the curing behavior are vapor-phase chromatography, nuclear magnetic resonance, and torsional braid analysis.

Differential Scanning Calorimetry (DSC) technique measures the instantaneous heat, Q, from a reactive sample as a function of temperature; it can be used directly, accurately and fast to study the rate of cure from the reaction heat. Assuming that the exothermic heat during cure is proportional to the extent of monomer conversion, cure kinetics and physical information can be estimated from dynamic and isothermal DSC tests.[34–44] Therefore, the reaction can be monitored using a relationship between heat and curing degree, $c = Q/Q_T$ (where Q_T is the total heat released during a reaction). The cure kinetics, dc/dt, is then defined as follows

$$\frac{dc}{dt} = \frac{\dot{Q}}{Q_T} \tag{2}$$

where $\dot{Q}$ is the instantaneous heat rate.

Typically, a DSC measurement is done at constant temperature, the isothermal test, or at a constant temperature rate, the dynamic test. However, there are different experimental setups to determine cure kinetic from DSC data. For instance, in Van Mele and coworkers[45–48] the reaction kinetics of epoxy-amine mixtures was monitored using quasi-isothermal Temperature Modulated Differencial Scanning Calorimetry (TMDSC), complemented by a nonisothermal postcure TMDSC experiment that provides additional real-time information on the reaction. Jenniger et al.[49] and Schawe[50] performed DSC and TMDSC to get a better understanding of the curing process. They used isothermal curing experiments and estimated the curing time dependence of conversion from the heat flow measurements. The authors used model-free kinetics (isoconversional methods) to evaluate the chemically controlled kinetics. The final conversion was found to determine how the curing temperature changes and the glass transition temperature during the cure was obtained. A phenomenological expression was introduced which is independent from the reaction temperature with a single parameter considered as the width of the glass transition. Mondragon and coworkers[51–55] proposed an iso-conversional kinetic analysis monitoring how the glass transition temperature changes with the degree of conversion for different thermosetting resins. The kinetically controlled region was described satisfactorily by a second-order kinetic equation and by an m-order ($m < 1$) equation after the vitrification is reached.

A convenient summary of the changes occurring during cure of a thermosetting system and to understand relationships between the conditions of cure and material behavior is the time–temperature–transformation (TTT) diagram. It was first described by Gillham and coworkers.[32,34,43,56–58] A typical TTT diagram is shown in Figure 2. It shows the different material states and characterizes the changes in the material during an isothermal cure as a function of time. Material states include liquid, sol-glass, sol/gel-rubber, gel-rubber, sol/gel-glass, gel-glass, and char. The glass transition temperature (T_g) of the material is used as

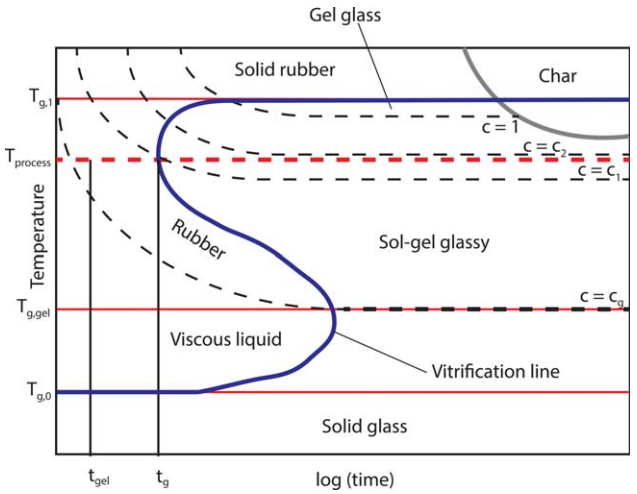

Figure 2. Schematic TTT diagram.[34,43,56–58] [Color figure can be viewed in the online issue, which is available at wileyonlinelibrary.com.]

a parameter to monitor the curing reaction. The unreacted material corresponds to $T_g = T_{g,0}$, essentially no reaction occurs because the reactive species are immobilized in the glassy state; the fully reacted material corresponds to $T_g = T_{g,1}$, where the resin is fully cured and it is represented by $c = 1$. The various changes occurring in the material during isothermal cure are characterized by contours of the time to reach a characteristic state. Each of these is marked by dramatic changes in the resin thermomechanical properties. For example, when the crosslinking starts the material turns from a viscous liquid to an elastic gel; this point is known as gel point ($T_{g,gel}$). This point is critical in the manipulation of thermosets because after that the material does not flow and it cannot be processed. The gel point occurs at a fixed extend of conversion ($c = c_g$ in the figure), this reaction mechanism is not a function of temperature. Gelation indicates the times required for a system to form an incipient, infinite molecular network that gives rise to long range elastic responses at a processing temperature, $T_{process}$. Another phenomenon occurs when the material changes from a viscous liquid or an elastic gel to a vitreous state, a point known as vitrification point. In this case, the glass transition temperature T_g, becomes equal to the curing processing temperature $T_{process}$. Near the vitrification, the local viscosity affects the kinetics, which in turn is a function of the extent of reaction and temperature. Thus, the cessation of reaction is not necessarily an indication that the reaction is complete, that is, the reaction may have been quenched due to vitrification and diffusion is now the control mechanism of the reaction. Subsequent exposure to temperatures greater than the temperature of cure could result in further reaction. The S-shaped curve is the vitrification curve and it shows $T_{process}$ as a function of the required time to reach the vitrification point. The liquid region is bounded by gelation (above $T_{g,gel}$) and vitrification (below $T_{g,gel}$). The gel rubber region is bounded by gelation and vitrification (above $T_{g,gel}$) in the absence of degradation, and char formation in the presence of degradation.

In this work, we provide an experimental and theoretical approach to analyze the cure kinetics of a linseed EP, at two different hardener concentrations, using DSC data only. Dynamical and a novel dynamic/isothermal DSC tests are used to obtain parameters for an auto-catalytic Kamal–Sourour model. This model is then used to simulate different processing conditions, resulting in a TTT diagram. This article is organized as follows: Materials and Methods section describes the materials and methods used to characterize the curing reaction. Cure Kinetics and TTT Algorithm section presents the methodology used to model the reaction kinetics and the integration method to obtain the TTT diagram. Results section presents the results for two EPs. Finally, a list of the main conclusions is summarized at the end.

MATERIALS AND METHODS

EP Description and Preparation

A linseed EP provided by IF Technologies LLC is used. This EP is considered as based-on-renewable-resource resin.[59,60] It contains at least two internal epoxide groups, which will crosslink by attaching molecules internally to one another, creating branches that may extend into crosslinked networks. Contrary to bifunctional terminal groups-epoxies, the hardener is the key material to form a crosslinked network. However, hardener is required to have functionalities greater than two to generate branching that may lead to crosslinking. The used linseed resin has been epoxidized and used in an epoxidized form by reacting it with polycarbonic anhydrides to induce the crosslinking reaction.

The mixture was prepared as follows: the linseed resin is mixed with the high temperature accelerator using a static mixer with 13 elements, two different hardener concentrations are used: 3 and 5% wt. These concentrations are the minimum and maximum concentrations recommended by the provider. After mixing, the samples were cooled using liquid nitrogen and kept cold before the DSC measurements at −12°C.

DSC Measurements

A Netzsch DSC 200 PC instrument, with a corresponding data acquisition and control system, was used to measure the T_g and the peak of the curing reaction using dynamic and isothermal experiments. The instrument operated with a nitrogen flow rate of about 20 mL/min through the cell. An empty pan was used as a reference. For the dynamic experiments, samples between 10 and 20 mg where placed inside hermetic aluminum pans and heated to 260°C using four different heating rates: 1, 2.5, 5, and 10°C/min. The calibration is done following Netzsch guidelines according to the heating rate. Three different heating/cooling cycles are done to identify the melting point of Hg (−18.87°C), In (156.6°C), Sn (231.9°C), Bi (271.3°C), Zn (419.5°C), and CsCl (645°C). These materials are provided reference materials in the device. For each melting peak, the maximum point is obtained; the values are averaged and entered in the software calibration option.

To obtain the T_g and to capture a diffusion-controlled mechanism, a novel experimental setup was performed. First, the samples were cooled down to −100°C and heated to 25°C at a rate of 2.5°C/min. Then, isothermal measurements were made to determine the rate of heat as a function of time; samples are then heated to a

specific curing temperature using a 5°C/min rate. This temperature is held for 3 h. After curing each specimen was heated again at 260°C to ensure a complete transformation and the process is repeated to obtain the baseline of the experiment. Figure 3(a) shows the DSC thermogram, where two sections are delimited, the first one is the actual experiment while the second one is for the generation of the baseline. The isothermal curing was performed at three different temperatures, 120, 140, and 160°C for the lower hardener concentration and four different temperatures, 120, 140, 160, and 180°C for the higher hardener concentration.

This new experimental ramp is used to avoid the typical difficulties of isothermal tests, where the rapid heating of the sample generates uncertainties in the initial part, thereby inducing errors during the heat evolution. It allows the generalization of the method previously proposed by Hernández-Ortiz and Osswald,[23,26–28] where isothermal difficulties were solved using dynamic DSC data. However, this method is applicable for materials that do not undergo diffusion-controlled mechanisms during reaction, that is, silicon rubbers. The proposed methodology in this article, extracts fundamental information from dynamic tests and from the novel dynamic/isothermal ramps.

The DSC data obtained from the dynamic and isothermal experiments were analyzed using the Netzsch DSC analysis software (Proteus), where additional treatment for the isothermal experiments was needed. Using the subtract tool of the software, the baseline obtained in the second run of the isothermal experiment is subtracted from the first run of the experiment to find the real peak of curing. Figure 4 shows the resultant DSC experiment.

CURE KINETICS AND TTT ALGORITHM

The DSC experiments provides the degree of cure, $c(t)$, and the cure evolution, dc/dt; the kinetics is then modeled with a transformation equation and the parameters, for such expression, are obtained numerically. Kinetic analysis of thermoset cure involves a proper selection for the kinetic model that fits the experimentally observed behavior. The required kinetics, evaluated by DSC, assumes that the reaction rate, dc/dt, is directly proportional to the rate of heat generation during the exothermic cure reaction (ordinate of DSC curve).[26,48,61–63]

The most used expressions are essentially semiempirical in nature, whereas others are based on the detailed chemical mechanisms of the thermosetting cure (mechanistic models). Essentially mechanistic models are intrinsically more complex and more difficult to implement than empirical models. In empirical models, the kinetic expressions, that is, the rate of cure is described by a set of rate constants. In general, a kinetic model relates the rate of conversion to some function of c and T. It is a common assumption that the functional dependence on c is separated from the dependence on T, so that the basic rate equation is[23,61,64,65]

$$\frac{dc}{dt} = k(T)f(c) \tag{3}$$

where

$$k(T) = Ae^{-\frac{E}{RT}} \tag{4}$$

E is the activation energy, A is the frequency factor, R is the universal gas constant, and T is temperature. This equation is known as Arrhenius equation. With regard to $f(c)$, there are several models used in the literature for the kinetics of thermosets during cure.[64–69] There are phenomenological, mechanistic models and those that attempt to follow complicate reaction kinetics. Any model can, in principle, be used for the fitting methodology proposed in this work. The curing model selection can be done according to particular preferences or depending of the thermosetting material.

In particular, for this article, the semiempirical auto-catalytic Kamal–Sourour model[17,70] was selected. It is a widely used model for EPs[6,26–28,31,38,71,72] and is defined as follows,

$$\frac{dc}{dt} = (k_1 + k_2 c^m)(1-c)^n \tag{5}$$

where m and n are the orders of reaction, c is the degree of cure, and k_i are rate constants, described by Arrhenius expressions. The first rate constant (k_1) characterizes the initial reactivity including the effect of catalysts, while the second (k_2) characterizes the auto-catalytic effect of the groups generated during the reaction. We used this model accounting for its applicability for the EPs and other type of thermosetting and elastomeric materials.

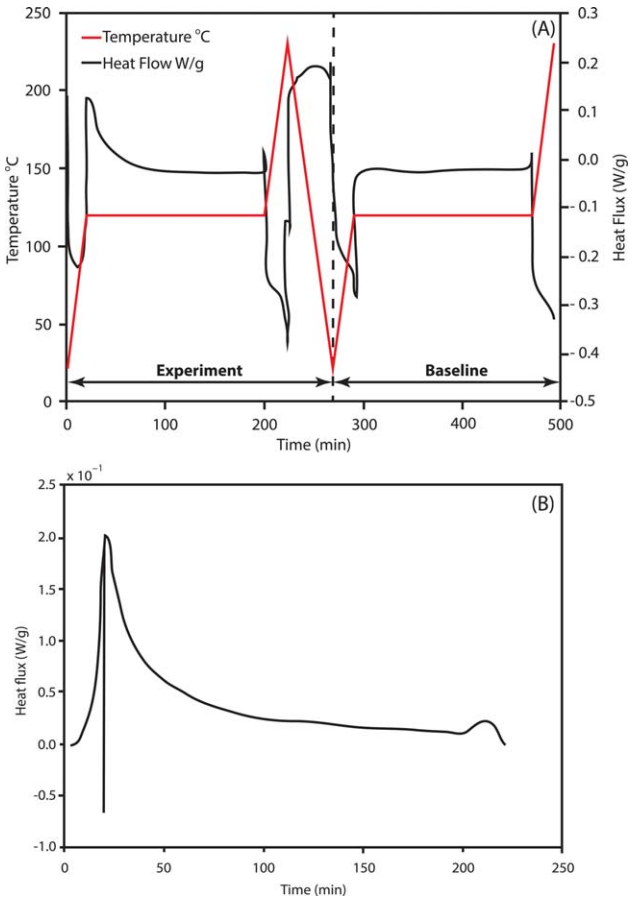

Figure 3. Novel Dynamic/Isothermal DSC thermogram: (A) experimental ramp including the baseline subtraction; (B) DSC thermogram after the baseline subtraction. [Color figure can be viewed in the online issue, which is available at wileyonlinelibrary.com.]

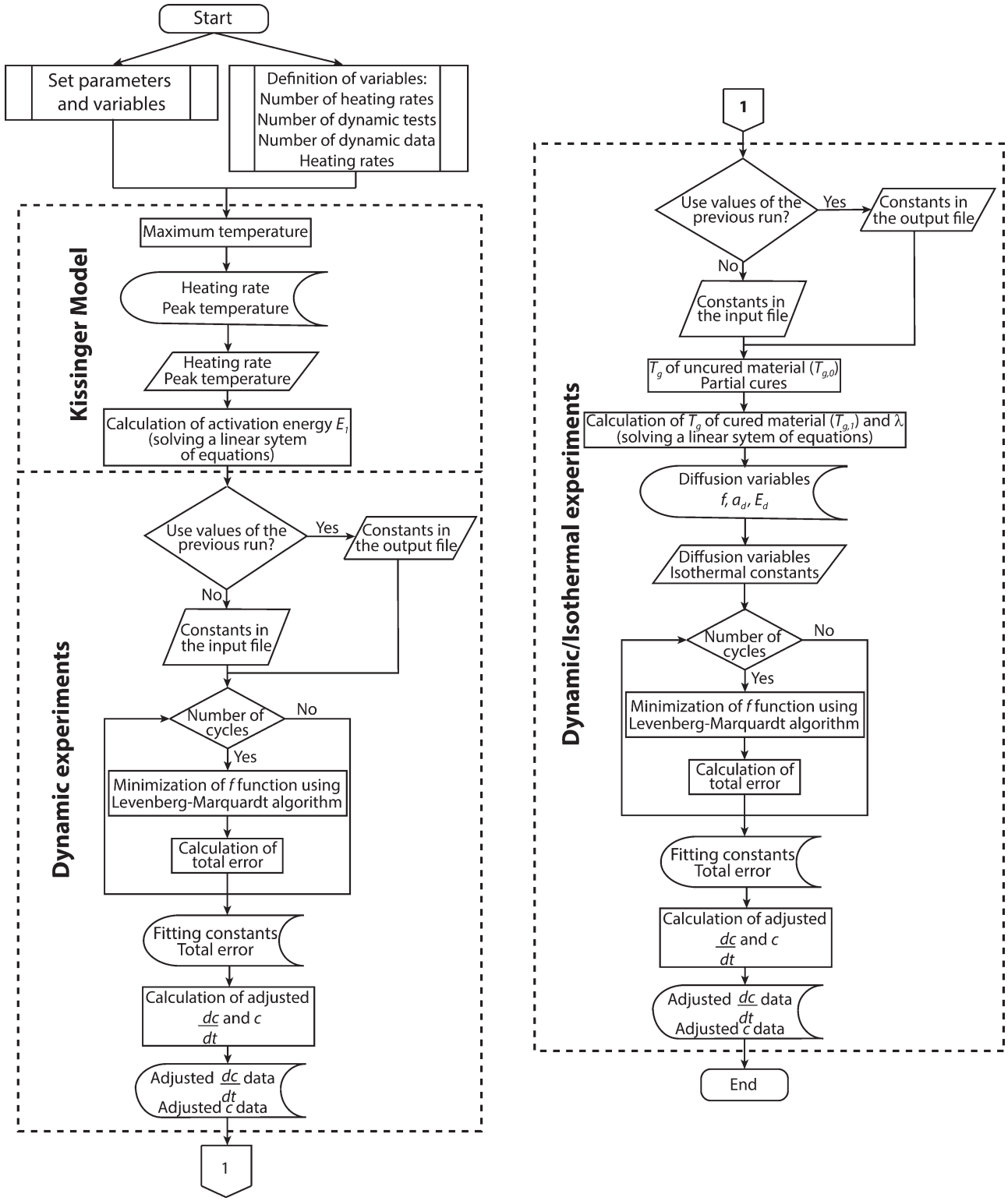

Figure 4. Schematic algorithm flowchart for fitting methodology.

This study uses the numerical methodology proposed by Hernández-Ortiz and Osswald[26] to find the kinetic parameters using dynamical DSC data. The methodology started from the work of Hadiprajitno et al.,[27] who used a nonlinear regression fit to obtain the kinetic parameters from isothermal DSC data. However, the authors realized that significant part of the information was lost during the initial temperature ramp. In addition, they found that most kinetic parameters were temperature dependent. From this work, Hernández-Ortiz and Osswald developed a numerical method[27] that, instead of fitting the kinetics parameters directly, it would seek for polynomial coefficients of temperature dependent expressions, using dynamic DSC

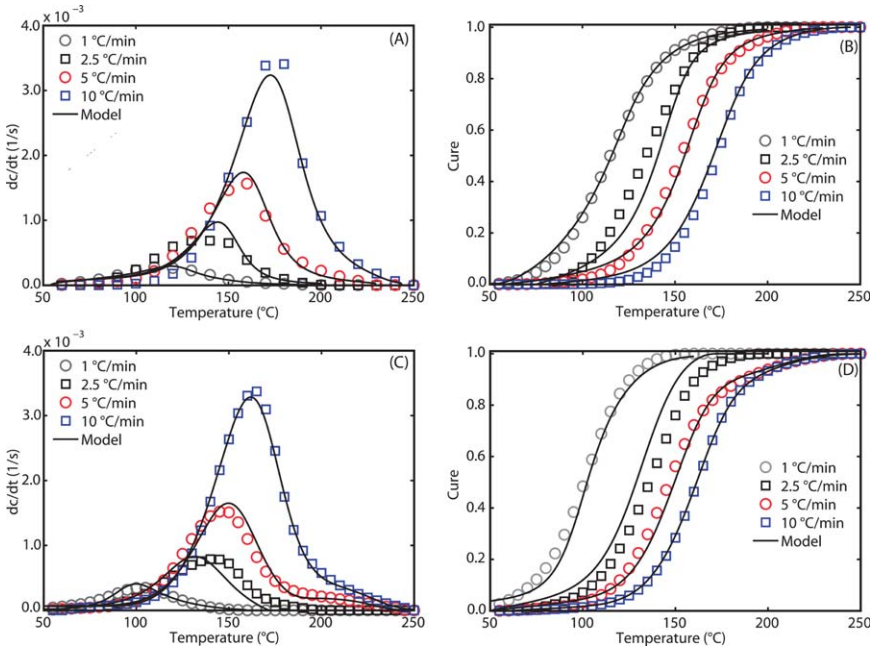

Figure 5. Dynamic DSC fittings for the aliphatic EPs: (A) curing rate and (B) cure degree for an epoxy with 3% wt. hardener; (C) curing rate and (D) cure degree for an epoxy with 5% wt. hardener. In these fittings the diffusion-controlled reaction mechanism is not included because during a dynamic DSC experiment the reactions progresses until the reactants are consumed. [Color figure can be viewed in the online issue, which is available at wileyonlinelibrary.com.]

data only. The method was used by Hernández-Ortiz and Osswald[23,73] and by Lopez et al.[28] to characterize the curing reaction of phenolic and silicone rubber materials. In these works, the authors realized that the fitting process was improved when a physically relevant activation energy is obtained directly from the measurements. Recall that in a numerical fitting, the kinetic parameters are numerical values with meaningless significance. Therefore, they included a methodology proposed by Kissinger[74,75] to obtain one activation energy (see Appendix A). The other kinetic parameters are fitted to the data retrieved from the DSC measurements via a nonlinear least-squares algorithm developed by Marquardt[76] and Levenberg.[77] Details of the numerical implementation are in the Appendix B.

The six parameters in the Kamal–Sourour (auto-catalytic) model, namely a_1, a_2, E_1, E_2, m, and n can be fitted to the experimental DSC data. The Kamal–Sourour parameters to be fitted are:

$$x=\{\, m \quad n \quad a_1 \quad E_1 \quad a_2 \quad E_2 \,\} \tag{6}$$

As mentioned, the first activation energy, E_1, is determined through the Kissinger kinetic model. The idea behind this selection is to found a physical meaningful value for E_1, representing the change of the curing reaction peak with the heating rate (the maximum reaction rate occurs at T_{peak}). Correspondingly, the activation energy, E_2, is also considered constant. The remaining parameters a_1, a_2, m, and n are the new targets for the nonlinear minimization; with the additional consideration that each of them is a function the temperature. It is assumed that this dependence follows a polynomial expansion, that is,

$$x_i=a_{i1}+a_{i2}\,T+a_{i3}\,T^2+\sigma(T^3) \tag{7}$$

where $i=1,\ldots,4$ and the components, a_{ij}, of a matrix $\mathbf{A}$ are the new targets for the fitting:

$$\mathbf{x}=\begin{pmatrix} m \\ n \\ a_1 \\ a_2 \\ E_2 \end{pmatrix}=\begin{bmatrix} a_{11} & a_{12} & a_{13} \\ a_{21} & a_{22} & a_{23} \\ a_{31} & a_{32} & a_{33} \\ a_{41} & a_{42} & a_{43} \\ E_2 & 0 & 0 \end{bmatrix}\begin{pmatrix} 1 \\ T \\ T^2 \end{pmatrix}+\sigma(T^3) \tag{8}$$

Notice that a_{ij} provide expressions for the kinetic parameters in the Kamal–Sourour model. However, these parameters do not

Table I. Kamal–Sourour Model Constants Obtained in Dynamic Experiments for an Aliphatic Epoxy Resin with 3% wt. Hardener

Parameter	Value	Units
a_1	$1.51 \times 10^4 - 7.90 \times 10^1 T + 1.04 \times 10^{-1} T^2$	s^{-1}
E_1	4.30×10^4	kJ/mol
a_2	$-7.09 \times 10^3 + 3.45 \times 10^1 T - 4.24 \times 10^{-2} T^2$	s^{-1}
E_2	3.76×10^4	kJ/mol
m	$-4.11 \times 10^1 + 1.97 \times 10^{-1} T - 2.15 \times 10^{-4} T^2$	-
n	$-5.85 \times 10^1 + 2.53 \times 10^{-1} T - 2.70 \times 10^{-4} T^2$	-

Table II. Kamal–Sourour Model Constants Obtained in Dynamic Experiments for an Aliphatic Epoxy Resin with 5% wt. Hardener

Parameter	Value	Units
a_1	$2.80 \times 10^4 - 1.52 \times 10^2 T + 2.07 \times 10^{-1} T^2$	s^{-1}
E_1	4.25×10^4	kJ/mol
a_2	$-2.04 \times 10^1 + 1.08 \times 10^{-1} T - 1.40 \times 10^{-4} T^2$	s^{-1}
E_2	1.05×10^4	kJ/mol
m	$2.45 \times 10^1 - 1.35 \times 10^{-1} T + 1.96 \times 10^{-4} T^2$	-
n	$4.48 \times 10^1 - 1.86 \times 10^{-1} T + 1.97 \times 10^{-4} T^2$	-

have a physical meaning, they provide a numerical fit to the behavior provided in the range of experiments. There are, in consequence, "good" and "bad" fittings, a touch of sense that is obtained with experience. Some tips of guidelines can help to find the "good" fits, for example, it is recommendable that the coefficients in the polynomial expansion decrease as the order of the polynomial increases. Fittings where the coefficients do not decrease can be improved by increasing the order of the polynomial interpolant.

The Kamal–Sourour model will accurately predict the degree of cure during the first stage of the reaction. However, at later stages of cure, once the reaction if controlled by diffusion the model will overpredict the degree. When the reaction is controlled by diffusion, the mobility of chemical reactants and active ends becomes the limiting step. Following the TTT diagram in Figure 2, the rational behind this is that before the vitrification line the mobility of reactants and chains is high, once the glass transition temperature is equal to the processing temperature (vitrification), the mobility decreases abruptly, and thermal motion (diffusion) will serve as the limiting mechanism for the reaction. Modifying the rate constants in the Kamal–Sourour model includes the diffusion-controlled kinetics. This was first proposed by Rabinowitch,[78] defining overall rate constants:

$$\frac{1}{k_i} = \frac{1}{k_{i,c}} + \frac{1}{k_d} \tag{9}$$

where k_i is the new rate constant of the ith reaction, $k_{i,c}$ is the Arrhenius dependent rate constant, and k_d is the diffusion rate constant, which is defined as follows

$$k_d = a_d e^{\left(-\frac{E_d}{RT}\right)} e^{\left(-\frac{b}{f}\right)} \tag{10}$$

where a_d and b are adjustable parameters, E_d is the activation energy for the diffusion process, and f is the equilibrium fractional free volume given by

$$f = 0.00048(T - T_g) + 0.025 \tag{11}$$

where T_g is the instantaneous glass transition temperature during cure. For $k_d \gg k_{i,c}$, which is the case prior to vitrification, the overall rate constant is governed by the Arrhenius rate

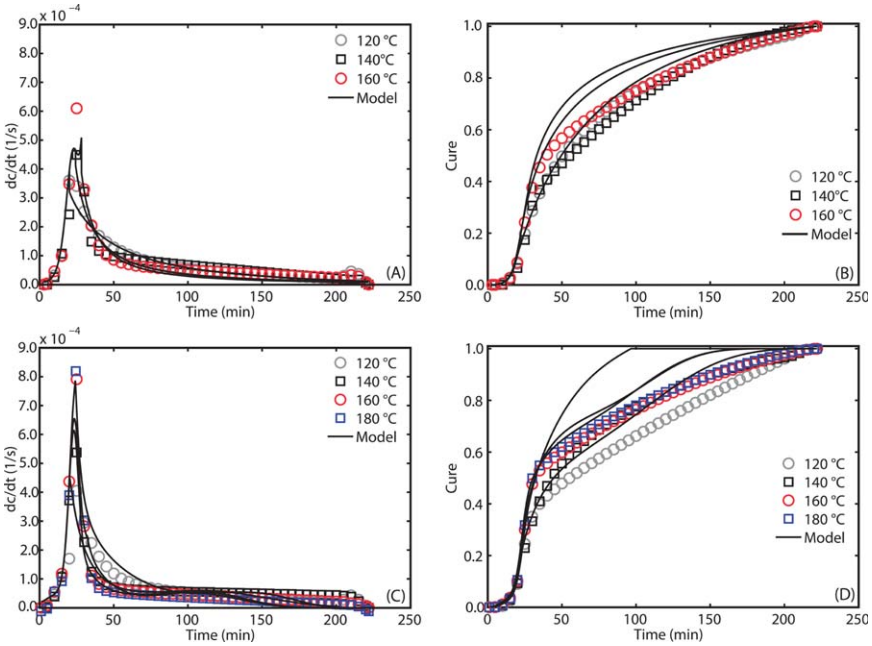

Figure 6. Dynamic/isothermal DSC fittings for the aliphatic EPs: (A) curing rate and (B) cure degree for an epoxy with 3% wt. hardener; (C) curing rate and (D) cure degree for an epoxy with 5% wt. hardener. In these fittings, the diffusion-controlled reaction mechanism is not included, resulting in poor fittings. [Color figure can be viewed in the online issue, which is available at wileyonlinelibrary.com.]

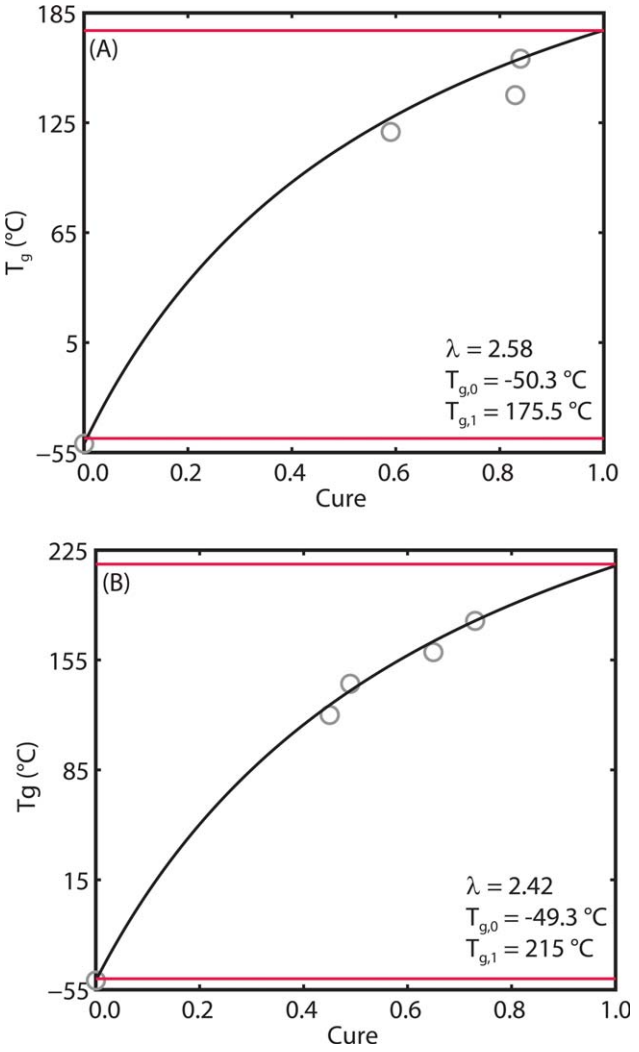

Figure 7. Experimental *Tg* and DiBenedetto's equation: (A) EP with 3% wt. hardener; (B) EP with 5% wt. hardener. [Color figure can be viewed in the online issue, which is available at wileyonlinelibrary.com.]

constant, and for $k_d \ll k_{i,c}$, which is the case after vitrification, the overall rate constant is governed by the diffusion rate constant.

An extra relationship is required for the glass transition temperature, where a unique one-to-one relationship between the glass transition temperature and conversion can be made. This is commonly done using the DiBenedetto's equation,[79] that is,

$$T_g = T_{g,0} + \frac{(T_{g,1} - T_{g,0})\lambda c}{1-(1-\lambda)c} \quad (12)$$

where $T_{g,0}$ is the glass transition temperature of the noncured resin, $T_{g,1}$ is the glass transition temperature of the fully reacted network, and λ is a structure dependent parameter, defined by $\lambda = \Delta C_{p,1}/\Delta C_{p,0}$, where ΔC_p is the difference in heat capacity between the glassy and rubber state for each state of cure.

RESULTS

An algorithm and a computer software were developed implementing the nonlinear regression fitting technique for the cure kinetics and to generate the TTT diagrams. Figure 4 shows the algorithm schematic representation to perform the fitting. Full implementation of the algorithm was done in Fortran, minimization package MINPACK (netlib.org) was used. Codes and routines are available for free download.

The total transformation heat, Q_T, is determined for the EP at both hardener concentrations as the area below the curing curve at a dynamic temperature ramp. For the EP with 3% wt. Q_T = 246.71 J/g, while for 5% wt. Q_T = 253.93 J/g. The total heat of reaction remained constant at each of the concentration over multiple heating rates. For each rate, three individual replicate runs were performed and the value of the standard deviation was ±3.58 J/g for the 3% wt. epoxy, while ±2.17 J/g for 5% wt. one.

Figure 5 shows DSC dynamic experiments and fittings for both the EPs. In this fitting, the diffusion-controlled mechanism is not included because during a dynamic experiment the reaction progresses until the reactants are consumed (notice how the cure degree always reaches 1.0). All dynamic scans had a similar shape, and there is an excellent agreement between the model and the experiments. The absolute error in the fitting was 7.07 × 10−7 for the 3% wt. epoxy and 8.98 × 10−7 for the 5% wt. epoxy. Tables I and II list the values for the polynomial coefficients of each kinetic parameter. After Q_T is measured and the dynamic DCS fittings are performed, we proceed to seek for the kinetic parameters of the dynamic/isothermal experiment [see Figure 3(a)]. The results for two EPs are shown in Figure 6. In the figure, it can be seen how the model is not able to follow the experiments. The reason is that the Kamal–Sourour model cannot, by itself, account for diffusion-controlled kinetics. Therefore, it is necessary to modify the model to account for these diffusive effects to accurately predict the degree of cure at late stages of processing. Notice that if the processing temperature is always higher than the glass transition temperature, the effects of diffusion can be neglected. Some thermosetting and elastomeric materials follow this physics; however, EPs are commonly processed under conditions that include diffusion control reaction kinetics.

Before the diffusion-controlled mechanism is included by modification to the reaction rates, the glass transition temperature as a function of cure must be fitted as well (DiBenedetto's equation). The values for the glass transition temperature are selected from the isothermal part of the test: for each temperature the rate of cure will decrease dramatically, indicating the diffusion-control mechanism dominance and the corresponding cure degree for that glass transition temperature. Figure 7 shows the fitting for DiBenedetto's equation. The points are T_g values obtained in the isothermal DSC experiments, while the continuous lines are DiBenedetto's equation. The parameter λ was obtained using a nonlinear regression fit, with an additional correction that ensures that the fitted $T_{g,1}$ cannot be higher than the experimental value.

Once diffusion is included, the model can represent the experimental observations. Figure 8 shows the curing rate and the degree of cure for the EPs considering diffusion. The agreement is now entirely satisfactory. Tables III and IV list the polynomial coefficients for the complete fitting; it includes the kinetic

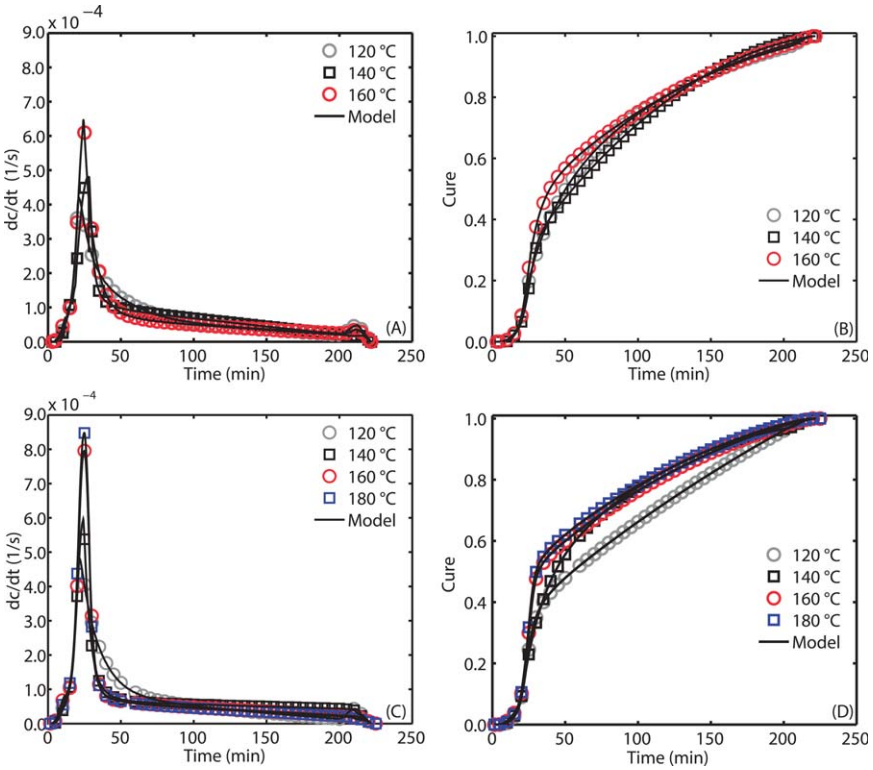

Figure 8. Dynamic/isothermal DSC fittings for the aliphatic EPs: (A) curing rate and (B) cure degree for an epoxy with 3% wt. hardener; (C) curing rate and (D) cure degree for an epoxy with 5% wt. hardener. In these fittings, the diffusion-controlled reaction mechanism is included. [Color figure can be viewed in the online issue, which is available at wileyonlinelibrary.com.]

parameters from the Kamal–Sourour and the diffusion control reaction parameters.

The complete kinetic fitting is used to build the TTT diagrams. First, at a specific temperature the cure is resolved by direct integration for 50,000 h to get as much information as possible. Then, the times in which cure values are 0.1, 0.2, 0.3, 0.4, 0.5, 0.6, 0.7, 0.8, 0.9, and 1.0 are identified; these isoconversion curves are plotted in a temperature versus time diagram. DiBenedetto's equation is used to calculate the glass transition temperature as a function of cure; these are included in the diagram to represent the vitrification line of the material. Figure 9 presents the TTT diagrams for the EP at the two hardener concentrations. When $T_c < T_{g,1}$, isothermal curing undergoes two different stages. The first one is controlled by the chemical reactivity of functional groups; the curing reaction takes place in the liquid state, and the T_g of the system is lower than the T_c. The reaction rate depends on T_c, until $T_c = T_g$. At this point, the second stage of curing starts. The system vitrifies, and the reaction decreases considerably until the reaction becomes

Table III. Kamal–Sourour Model Constants Modified with Diffusion Parameters Obtained in Dynamic/Isothermal Experiments for an Aliphatic Epoxy Resin with 3% wt. Hardener

Parameter	Value	Units
a_1	$4.00 \times 10^4 - 2.34 \times 10^1 T + 3.52 \times 10^{-1} T^2$	s^{-1}
E_1	4.30×10^4	kJ/mol
a_2	$-2.72 \times 10^3 + 6.52 \times 10^6 T - 4.24 \times 10^{-2} T^2$	s^{-1}
E_2	9.99×10^4	kJ/mol
m	$2.55 \times 10^0 - 1.25 \times 10^{-5} T + 2.86 \times 10^{-8} T^2$	-
n	$-1.95 \times 10^0 + 8.72 \times 10^{-4} T - 1.94 \times 10^{-5} T^2$	-
λ	2.58	--
b	$-1.93 \times 10^{-1} + 8.72 \times 10^{-4} T - 1.94 \times 10^{-5} T^2$	--
a_d	$1.76 \times 10^{-1} - 7.93 \times 10^{-2} T + 8.94 \times 10^{-4} T^2$	s^{-1}
E_d	-8.83×10^{-7}	kJ/mol

Table IV. Kamal–Sourour Model Constants Modified with Diffusion Parameters Obtained in Dynamic/Isothermal Experiments for an Aliphatic Epoxy Resin with 5% wt. Hardener

Parameter	Value	Units
a_1	$1.52 \times 10^4 - 8.46 \times 10^1 T + 1.18 \times 10^{-1} T^2$	s^{-1}
E_1	4.25×10^4	kJ/mol
a_2	$2.43 \times 10^{23} - 6.56 \times 10^{-12} T - 1.28 \times 10^{-14} T^2$	s^{-1}
E_2	1.86×10^5	kJ/mol
m	$-1.80 \times 10^1 + 1.95 \times 10^{-4} T - 5.87 \times 10^{-16} T^2$	-
n	$-6.24 \times 10^1 - 2.60 \times 10^{-1} T - 2.45 \times 10^{-4} T^2$	-
λ	2.42	-
b	$5.84 \times 10^{-2} + 3.26 \times 10^{-5} T + 2.92 \times 10^{-6} T^2$	-
a_d	$-1.35 \times 10^0 - 5.90 \times 10^{-3} T - 7.24 \times 10^{-4} T^2$	s^{-1}
E_d	8.86×10^4	kJ/mol

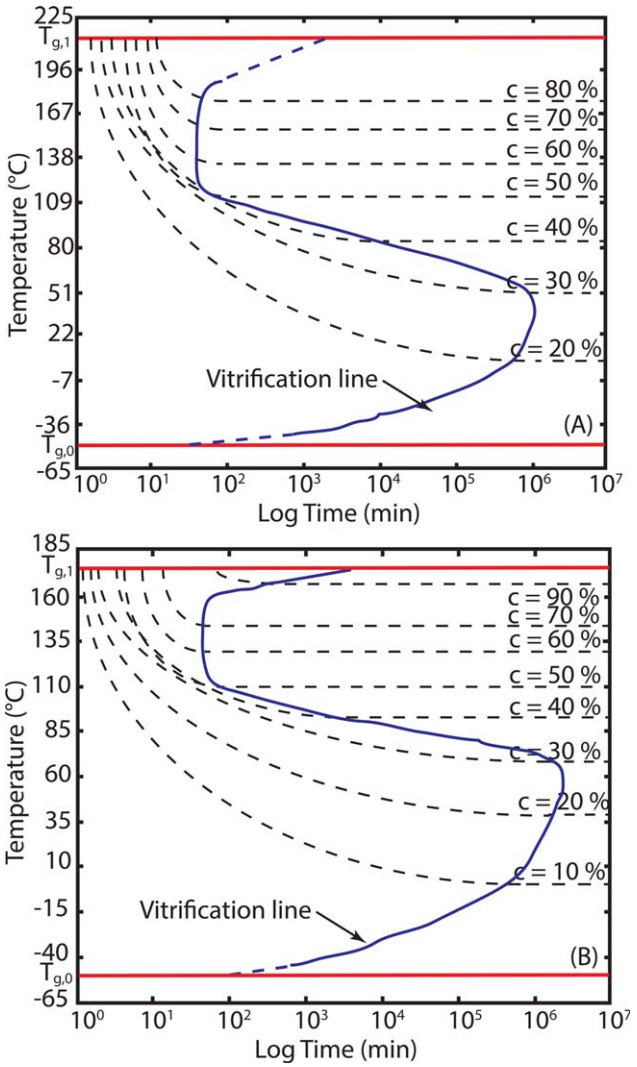

Figure 9. TTT diagrams: (A) EP with 3% wt. hardener; (B) EP with 5% wt. hardener. [Color figure can be viewed in the online issue, which is available at wileyonlinelibrary.com.]

practically inhibited by a restricted reacting groups mobility, which prevents full conversion. The reaction time required for reaching $T_c = T_g$, is called vitrification time t_v. The increase of the hardener concentration affects slightly the $T_{g,0}$ (only 1°C) but it has an important effect in $T_{g,1}$, changing from 175.5°C for the 3% wt. hardener to 215°C for 5% wt. Besides, a 5% wt. concentration causes early vitrification.

CONCLUSIONS

The cure kinetics of linseed EP with two different hardener concentrations was studied. It indicates that only one reaction occurs over the complete cure in the temperature range 20–250°C. Isothermal experiments performed by DSC indicate the reaction is controlled by diffusion and show time dependent rate of heat evolution of the epoxy material. At the beginning, there is an increase in the slope corresponding to the dynamical part of the experiment, after that the curves show the time dependent rate of heat evolution of an epoxy sample. The existence of a peak in each isothermal curve suggests the catalytic effect of the chemical groups present in the reaction products. A decrease in the rate of the curve was observed shortly after the peak. This phenomenon was more pronounced at the high concentration of accelerator. This change could be identified with the onset of a diffusion-controlled reaction mechanism due to the increased viscosity of the system. It can also be associated with the gel point and the formation of an infinite network.

The effect of diffusion control can be incorporated into the reaction kinetics by modifying the overall rate constant. During the course of isothermal curing, both in the kinetically and diffusion-controlled regimes, the overall rate constant is assumed to be a combination, in parallel, of the chemical rate constant and the diffusion rate constant. The temperature dependence of the kinetically controlled rate constant is given by the Arrhenius-type expression, whereas a modified form of the DiBenedetto's equation gives the diffusion-controlled rate constant. Calculation using such modified rate constants

provides good correlation with the experimental results at all cure temperatures.

ACKNOWLEDGMENTS

The authors wish to thank IF Technologies LLC for providing the resins used in this research, the Polymer Engineering Center and the Soft Materials Lab. at the University of Wisconsin-Madison for the use of facilities and the measurement instruments. JPHO and NCR are thankful to COLCIENCIAS and Extrusiones S.A. for the financial support of the cofunded project CT-102-2009, 111-845-422-036. JPHO would like to thank the Biotechnology Center at the University of Wisconsin-Madison for constant help in the experimental setup and computer resources.

APPENDIX A: KISSINGER'S MODEL

The Kissinger model[74,75] has been established for dynamical regime and shows the effects of time and temperature on the reaction. It starts with defining an order n kinetics,

$$\frac{dc}{dt}=k(1-c)^n \tag{A1}$$

where dc/dt is the change of conversion with time, c is concentration, n is the reaction order, and k is defined by

$$k=ae^{\left(-\frac{E}{RT}\right)} \tag{A2}$$

an Arrhenius equation where a is a factor, E is the activation energy, R is the universal gas constant, and T is the processing temperature. Including the Arrhenius expression in the kinetics will result in

$$\frac{dc}{dt}=ae^{\left(-\frac{E}{RT}\right)}(1-c)^n \tag{A3}$$

During the reaction, temperature rises and the reaction rate, dc/dt, will reach a maximum. Once the reactants are consumed the reaction rate will drop to zero. The maximum deflection in differential thermal analysis occurs in a temperature at which reaction rate is maximum; this temperature is defined by T_{peak} when $d/dt(dc/dt)$ is zero. Integrating by parts eq. (A3), an expression for the unreacted material is obtained, that is,

$$\frac{1}{1-n}\left(\frac{1}{(1-c)^{n-1}}-1\right)=\frac{aRT^2}{E\dot{T}}\left(1-\frac{2RT}{E}\right)e^{\left(-\frac{E}{RT}\right)} \tag{A4}$$

or better,

$$-\frac{E}{R}=\frac{d}{d(1/T)}\left(ln\frac{\dot{T}}{T_{peak}^2}\right) \tag{A5}$$

Therefore, the activation energy can be obtained as the slope of a line that relates rate of reaction with temperature.

Physically, the reaction occurs when the molecules have enough energy to overcome the barrier generated by the activation energy. When temperature increases, the number of molecules with enough kinetic energy is higher and the probability to overcome the energy barrier is higher. Assuming that the molecules follow a Maxwell–Boltzmann distribution, the fraction of molecules whose kinetic energy exceeds the activation energy can be inferred and it increases rapidly as the temperature is raised.

APPENDIX B: MATHEMATICAL MODEL AND NONLINEAR LEAST-SQUARES METHOD

Three vectors are needed from the DSC experiment at each reaction rate: temperature, degree of cure, and reaction rate:

$$T=\{T_1 \quad T_2 \quad \ldots \quad \ldots \quad T_{N-1} \quad T_N\}$$
$$c=\{c_1 \quad c_2 \quad \ldots \quad \ldots \quad c_{N-1} \quad c_N\}$$
$$\frac{dc}{dt}=\left\{\left(\frac{dc}{dt}\right)_1 \quad \left(\frac{dc}{dt}\right)_2 \quad \ldots \quad \ldots \quad \left(\frac{dc}{dt}\right)_{N-1} \quad \left(\frac{dc}{dt}\right)_N\right\} \tag{B1}$$

where N is the number of experimental data.

The basic idea behind every least-squares approximation is to minimize the mean squared difference between the experiments and the selected function by varying the coefficients that define such function, that is, the polynomial coefficients for the kinetic parameters in the Kamal–Sourour model. Because the function that is selected to fit the experimental data is nonlinear, regular least-squares method cannot be used. Levenberg and Marquardt[76,77] proposed a nonlinear fitting method that uses the fundamentals behind the Newton–Raphson method for the solution of nonlinear equations.[80,81] The nonlinear squares method starts, similar to nonlinear solvers, from an initial guess for the **A** matrix containing the polynomial coefficients; thus, the initial kinetic parameters are defined by

$$x_{0,i}=[\mathbf{A}]_0\{1 \quad T_i \quad T_i^2\} \tag{B2}$$

The idea is to find the minimum a function $f_i(x)$,

$$\min\left[\frac{1}{2}\sum_{i=1}^{N}f_i(x)^2\right] \tag{B3}$$

defined as follows

$$f_i(x)=\left(\frac{dc}{dt}\right)_i-\frac{dc}{dt}(\mathbf{x}_{0,i}) \tag{B4}$$

The **x** vector is updated in an iterative fashion, following the gradient given by the minimization function, assuming that the initial guess in contained within the global minima of $f_i(x)$:

$$x_k=x_{k-1}-[J(x_{k-1})^TJ(x_{k-1})+\kappa I]^{-1}J(x_{k-1})f(x_{k-1}) \tag{B5}$$

where $x_k=[A]_k\{1 \quad T \quad T^2\}$, **J** is the Jacobian, k the iteration step, and κ is parameter that controls the size of the updating step:

$$\kappa=0 \quad \text{if} \quad x_k-x_{k-1}\geq J(x_{k-1})^TJ(x_{k-1})^{-1}J(x_{k-1})^Tf(x_{k-1}) \tag{B6}$$

and $\kappa\in(0,\ 1]$ otherwise.

REFERENCES

1. Menges, G.; Osswald, T. A. Materials Science of Polymers for Engineers, 3rd Ed.; Hanser Gardner: Munich, Germany, **2012**.
2. Young, R. J.; Lovell, P. A. Introduction to Polymers; CRC Press: Boca Raton, Florida, **2011**.
3. Pascault, J. P.; Sautereau, H.; Verdu, J.; Williams, R. J. J. Thermosetting Polymers; CRC Press: Boca Raton, FL, **2002**.
4. Chern, G. W.; Poehlein, C.-S. *Polym. Eng. Sci.* **1987**, *27*, 788.

5. Ramis, X.; Salla, J. M. *J. Poly. Sci. Part B: Polym. Phys.* **1997**, *35*, 371.
6. Chiao, L.; Lyon, R. *J. Compos. Mater.* **1990**, *24*, 739.
7. Huang, Y.; Bao, T.; Wang, H. *Adv. Mater. Res.* **2013**, *1779*, 671.
8. Nicolais, L.; Borzacchiello, A.; Lee, S. M., Eds. Wiley Encyclopedia of Composites; Wiley: Hoboken, New Jersey, **2012**.
9. Ratna, D., Ed. Handbook of Thermoset Resins; iSmithers Rapra Publishing: Shrewbury, Shropshire, United Kingdom, **2009**.
10. Lu, M.; Shim, M.; Kim, S. *Polym. Eng. Sci.* **1999**, *39*, 274.
11. Akatsuka, M.; Takezawa, Y.; Amagi, S. *Polymer* **2001**, *42*, 3003.
12. Liu, L.; Wagner, D. *Compos. Sci. Technol.* **2005**, *65*, 1861.
13. Wang, H.; Bai, Y.; Liu, S.; Wu, J.; Wong, C. P. *Acta Mater.* **2002**, *50*, 4369.
14. Dutta, A.; Ryan, M. *J. Appl. Polym. Sci.* **1979**, *24*, 635.
15. Harsch, M.; Karger-Kocsis, J.; Holst, M. *Eur. Polym. J.* **2007**, *43*, 1168.
16. Sanchez, G.; Brito, Z.; Mujica, V.; Perdomo, G. *Polym. Degrad. Stab.* **1993**, *40*, 109.
17. Sourour, S.; Kamal, M. *Thermochim. Acta* **1976**, *14*, 41.
18. Kenny, J. M.; Maffezzoli, A.; Nicolais, L. *Compos. Sci. Technol.* **1990**, *38*, 339.
19. Mijovic, J.; Fishbain, A.; Wijaya, J. *Macromolecules* **1992**, *25*, 979.
20. Boey, F. Y. C.; Lye, S. W. *Composites* **1992**, *23*, 261.
21. Kenny, J. M. *Compos. Struct.* **1994**, *27*, 129.
22. Antonucci, V.; Giordano, M.; Hsiao, K.-T.; Advani, S. G. *Int. J. Heat Mass Transfer* **2002**, *45*, 1675.
23. Osswald, T. A.; Hernandez-Ortiz, J. P. Polymer Processing: Modeling and Simulation; Hanser Gardner: Munich, Germany, **2006**.
24. Asua, J. Polymer Reaction Engineering; Wiley-Blackwell: Hoboken, New Jersey, **2007**.
25. Christiansen, A. W.; Gollob, L. *J. Appl. Polym. Sci.* **1985**, *30*, 2279.
26. Hernandez-Ortiz, J.; Osswald, T. *J. Polym. Eng.* **2005**, *25*, 23.
27. Hadiprajitno, S.; Hernandez-Ortiz, J.; Osswald, T. Developing Time-Temperature- Transformation Diagramas for Unsaturated Polyesters Using DSC Data. In Society of Plastics Engineers, ANTEC 2003, Nashville, Tennessee, May **2003**.
28. Lopez, L.; Cosgrove, A.; Hernandez-Ortiz, J.; Osswald, T. *Polym. Eng. Sci.* **2007**, *47*, 675.
29. Jenkins, R.; Karre, L. *J. Appl. Polym. Sci.* **1966**, *10*, 303.
30. Kuznetsov, G.; Nikiforov, N.; Potekhin, R.; Kalinin, B.; Tarakanov, O. *Polym. Sci. USSR* **1975**, *17*, 2454.
31. Theriault, R. Modeling and Simulation of the Manufacturing of Copper-Clad Laminates; PhD thesis, University of Wisconsin-Madison, **1998**.
32. Enns, J.; Gillham, J. *J. Appl. Polym. Sci.* **1983**, *28*, 2567.
33. Vakil, U.; Martin, G. *J. Appl. Polym. Sci.* **1992**, *46*, 2089.
34. Pang, K.; Gillham, J. *J. Appl. Polym. Sci.* **1990**, *39*, 909.
35. Prime, R. *Polym. Eng. Sci.* **1973**, *13*, 365.
36. Peyser, P.; Bascom, W. *J. Appl. Polym. Sci.* **1977**, *21*, 2359.
37. Baron, J.; Wright, W. *Thermochim. Acta* **1985**, *85*, 415.
38. Charter, M.; Chataing, G.; Vergnaud, J. *Thermochim. Acta* **1985**, *85*, 135.
39. Khabenko, A.; Dolmatov, S. *J. Therm. Anal.* **1990**, *36*, 46.
40. Thiagaran, R.; Reddy, P.; Sridhar, S.; Ratra, M. *J. Therm. Anal.* **1990**, *36*, 277.
41. Focke, W.; Smit, M.; Tolmay, A.; Van der Walt, L.; Van Wyk, W. *Polym. Eng. Sci.* **1991**, *31*, 1665.
42. Monserrat, S. *J. Appl. Polym. Sci.* **1992**, *44*, 545.
43. Simon, S.; Gillham, J. *J. Appl. Polym. Sci.* **1992**, *46*, 1245.
44. Richardson, M. *Pure Appl. Chem.* **1992**, *64*, 1789.
45. Swier, S.; Van Mele, B. *Thermochim. Acta* **1999**, *330*, 175.
46. Swier, S.; Van Mele, B. *J. Polym. Sci. Part B: Polym. Phys.* **2003**, *41*, 594.
47. Swier, S.; Van Assche, G.; Vuchelen, W.; Van Mele, B. *Macromolecules* **2005**, *38*, 2281.
48. Swier, S.; Van Mele, B. *Macromolecules* **2003**, *36*, 4424.
49. Jenniger, W.; Schawe, J.; Alig, I. *Polymer* **2000**, *41*, 1577.
50. Schawe, J. *Thermochim. Acta* **2002**, *388*, 299.
51. Eceiza, A.; Zabala, J.; Egiburu, J.; Corcuera, M.; Mondragon, I.; Pascault, J. *Eur. Polym. J.* **1999**, *35*, 1949.
52. Blanco, M.; Corcuera, M.; Riccardi, C.; Mondragon, I. *Polymer* **2005**, *46*, 7989.
53. Kortaberria, G.; Arruti, P.; Gabilondo, N.; Mondragon, I. *Eur. Polym. J.* **2004**, *40*, 129.
54. Tejado, A.; Kortaberria, G.; Labidi, J.; Echeverri, J.; Mondragon, I. *Thermochim. Acta* **2008**, *471*, 80.
55. Tejado, A.; Kortaberria, G.; Pena, C.; Labidi, J.; Echeverria, J.; Mondragon, I. *Ind. Crops Prod.* **2008**, *27*, 208.
56. Chan, L.; Nae, H.; Gillham, J. *J. Appl. Polym. Sci.* **1984**, *29*, 3307.
57. Peng, X.; Gillham, J. *J. Appl. Polym. Sci.* **1985**, *30*, 4685.
58. Palmese, G.; Gillham, J. *J. Appl. Polym. Sci.* **1987**, *34*, 1925.
59. Moore, G. R.; Kline, D. E.; Blankenhorn, P. R. *Wood Fiber Sci.* **1983**, *15*, 223.
60. Mustapha, S. N. H.; Rahmat, A. R.; Arsad, A. *Rev. Chem. Eng.* **2013**, 1.
61. Martin, J.; Salla, J. *Thermochim. Acta* **1982**, *207*, 279.
62. Hojjati, M.; Hoa, S. *J. Compos. Mater.* **1995**, *29*, 1741.
63. Mondragon, I.; Solar, L.; Recalde, I.; Gomez, C. *Thermochim. Acta* **2004**, *417*, 19.
64. Kenny, J.; Apicella, A.; Nicolais, L. *Polym. Eng. Sci.* **1989**, *29*, 973.
65. Horie, K.; Hiura, H.; Sawada, M.; Mita, I.; Kambe, H. J. *Polym. Sci. Part A: Polym.* **1970**, *8*, 1357.
66. Loos, A.; Springer, G. *J. Compos. Mater.* **1983**, *17*, 135.
67. Sanford, W.; McCullough, R. *J. Polym. Sci. Part B: Polym. Phys.* **1990**, *28*, 973.
68. Cole, K. *Macromolecules* **1991**, *24*, 3093.
69. Cole, K.; Hechler, J.; Noel, D. *Macromolecules* **1991**, *24*, 3098.

70. Kamal, M.; Sourour, S. *Polym. Eng. Sci.* **1973**, *13*, 59.
71. Stutz, H.; Mertes, J.; Neubecker, K. *J. Polym. Sci. Part A: Polym. Chem.* **1993**, *31*, 1879.
72. Martin, J.; Cadenato, A.; Salla, J. *Thermochim. Acta* **1997**, *306*, 115.
73. Hernandez-Ortiz, J. P.; Osswald, T. A. *J. Appl. Polym. Sci.* **2011**, *119*, 1864.
74. Kissinger, H. *J. Res. Natl. Bur. Stand.* **1956**, *57*, 217.
75. Kissinger, H. *Anal. Chem.* **1957**, *29*, 1702.
76. Marquardt, D. *J. Soc. Ind. Appl. Math.* **1963**, *11*, 431.
77. Levenberg, K. *J. Appl. Math.* **1944**, *2*, 164.
78. Rabinowitch, E. *Trans. Faraday Soc.* **1937**, *33*, 283.
79. DiBenedetto, E. *Indiana Univ. Math. J.* **1983**, *32*, 83.
80. Trefethen, L. N.; Bau, D, III. Numerical Linear Algebra; SIAM: Philadelphia, **1997**.
81. Press, W. H.; Teukolsky, S. A.; Vetterling, W. T.; Flannery, B. P. Numerical Recipes in Fortran 77, 2nd ed.; Cambridge University Press: Cambridge, **1992**.